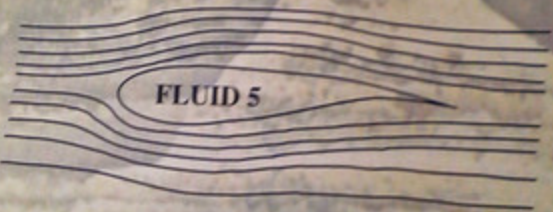


PROCEEDINGS OF
THE FIFTH INTERNATIONAL CONFERENCE
OF FLUID MECHANICS

ICFM5

January 2 - 5, 1995

CAIRO - EGYPT

A graphic consisting of several horizontal, wavy lines that converge and diverge to form a central oval shape. The text "FLUID 5" is centered within this oval.

FLUID 5



VOLUME II

PREDICTION OF ROUGH SURFACE THERMAL TURBULENT BOUNDARY LAYER

By

G.H.Abd Alla, K.M.El-Shazly, O.E.Abd-Ellatif &
M.F.Abd Rabbo

Zagazig University - Shoubra Faculty Of Engineering

ABSTRACT:

The convective heat transfer and skin friction drag for smooth and rough surfaces in zero and non-zero pressure gradient flows are investigated by solving the hydrodynamic and thermal turbulent boundary layer equations. The present procedure solves the governing equations using the implicit finite difference numerical algorithm. A modified mixing length model is used for the turbulent flow calculations. The computation scheme is improved by using the turbulence model wall function and a special procedure for evaluating the normal distance near the wall. For rough wall flows, further adjustments are achieved by using the equivalent sandgrain roughness. Comparisons with available experimental data are presented showing favourable agreement between present prediction and previously published measurements. It is found that, the skin friction coefficient (C_f) and Stanton number (St) for accelerated flows are greater than those for decelerated flows at the same roughness. Reynolds analogy factor correlations are predicted for turbulent flows over both smooth and rough surfaces.

1 INTRODUCTION

The majority of flows which occurs in nature or in engineering practice are turbulent. One example is the turbulent flow over a hot flat plate with and without pressure gradient. On the turbulent flow along a rigid wall, the turbulence and consequently both skin friction drag and heat transfer are affected by the wall, at least in the region close to the wall. For smooth wall, the turbulence is affected by the action of viscous stresses, while for a rough wall, the turbulence is affected by the action of induced

forces resulting from the flow around the roughness elements.

According to the experimental data, the turbulent boundary layer can be considered a composite layer made up of inner layer (wall region) and outer region. The existence of the two regions is due to the different response to shear stress and pressure gradient by the fluid near the wall. By assuming constant shear flux layer and the assumption of Prandtl [1] which relates the mixing length to the normal distance near the wall, it is found that the velocity profile in the inner layer is logarithmic. Van Driest [2] modified the equation of mixing length which including a non-dimensional damping factor in exponential term while, Cebeci and Chang [3] investigated another formula of mixing length but including the effect of roughness which displaced the y -coordinate by Δy and the velocity profile by a downward shift of Δu^* . The value of Δu^* is investigated by many authors [4,5] and found that it depends on the roughness height and the roughness density. Cebeci [6] extended the mixing length formula which is used in Van Driest model for flows with pressure gradient by deducing another definition of the damping factor. Spalding [7] deduced a single formula for the whole range of y in the wall region.

In the outer region, some investigators have shown that for large value of y , the logarithmic velocity distribution deviates from the actual velocity distribution so that the velocity defect law is used instead of logarithmic profile. Clauser [8] has shown that, the outer layer is more sensitive to pressure gradient than the inner layer, thus the velocity profile in the outer region depends on another pressure gradient parameter.

In the present work, the method of solution modified Spalding technique specially in some calculations of the turbulence model to include the effects of the pressure gradient and surface roughness on the skin friction coefficient (C_f) and Stanton number (St). The calculation of normal distance near the wall which was modified by Abd Rabbo

[9] is used in the present work. The wall function for heat transfer based on couette flow that was deduced by Ilegbusi and Jayatilaka [10], is used to calculate Stanton number (St) in the presence of flows over rough surfaces.

2 MATHEMATICAL FORMULATION AND NUMERICAL TECHNIQUE

It is assumed that the flow is parabolic, incompressible, steady and the boundary layer approximation is valid. The hydrodynamic and thermal turbulent boundary layer equations in cartesian coordinates are transformed to Von Mises ($x-\psi$) coordinates. It is found that there is a similarity between the two governing equations after they were transformed to Von Mises coordinates, thus the governing equations can be transformed to one equation in a general form. Spalding [7] transformed the general form of boundary layer equations to ($x-\omega$) coordinate system as shown in fig.(1). The governing equation is

$$\frac{\partial \phi}{\partial x} + (\alpha + b\omega) \frac{\partial \phi}{\partial \omega} = \frac{\partial}{\partial \omega} \left(c \frac{\partial \phi}{\partial \omega} \right) + d \quad (1)$$

The first term of the above equation represents the effect of longitudinal convection, the second term represents the effect of lateral convection, the third term represents the effect of effective viscous action (heat conduction or diffusion) and the fourth term represents the effect of generation and destruction where

$$a = \frac{m_1}{(\psi_K - \psi_1)}, \quad b = \frac{(h_K - h_1)}{(\psi_K - \psi_1)} \quad \text{and}$$

$\begin{matrix} C \\ \text{if } \phi = u \\ \text{if } \phi = h \end{matrix}$
 $\xrightarrow{\text{is a measure of the transport property}}$
 $\xrightarrow{C = \text{effective viscosity}}$
 $\xrightarrow{C = \text{effective thermal conductivity}}$

where u and h are the velocity and enthalpy of the flow

d $\xrightarrow{\text{represents the source term}}$

A 4-node implicit integration formula are used to derive the finite difference equations as shown in fig.(2). After discretization technique to equation (1), the equation

$$U_i U_{i,0} = A_i U_{i+1/2} + B_i U_{i-1/2} + C_i \quad (2)$$

The coefficients A_i, B_i, C_i and D_i are calculated for each nodal point from expressions obtained by integrating equation (1) over appropriate control volumes δx shown in fig. (3). The boundary conditions are

$$u = 0 \quad \text{at} \quad \omega = 0$$

$$u = U_\infty \quad \text{at} \quad \omega = 1$$

The coefficients of equation (2) can be deduced as follows:-

$$A_i = \left(T - \frac{1}{2} \dot{m} \right)_{i+1/2} \quad (3)$$

$$B_i = \left(T + \frac{1}{2} \dot{m} \right)_{i-1/2} \quad (4)$$

$$C_i = U_{i,0} \frac{(\psi_x - \psi_x)U}{\delta x} (\omega_{i+1/2} - \omega_{i-1/2}) + S_i \quad (5)$$

$$D_i = A_i + B_i + \frac{(\psi_x - \psi_x)U}{\delta x} (\omega_{i+1/2} - \omega_{i-1/2}) \quad (6)$$

where $T_{i+1/2} = \frac{(\mu_{eff})_{i+1/2}}{(\gamma_{i+1} - \gamma_{i-1})U}$, $T_{i-1/2} = \frac{(\mu_{eff})_{i-1/2}}{(\gamma_i - \gamma_{i-1})U}$ and $\dot{m} = (a + b\omega)(\psi_x - \psi_x)U = (1 - \omega) \dot{m}_1 + \omega \dot{m}_2$

The source term S_i of equation (5) is equal to the integration of the fourth term in equation (1) with respect to ω and the limits of integration are from $i-1/2$ to $i+1/2$. The finite-difference equations at each step of δx are derived and written as a set of equations. By using Gauss elimination method, these equations can be solved as follows:-

$$U_i = P_i U_{i+1} + Q_i \quad (7)$$

$$P_i = A_i / D_i$$

$$Q_i = \frac{A_i}{(D_i - B_i P_{i-1})} \quad i = 1, 2, \dots, n-1 \quad (8)$$

$$Q_n = \frac{(B_n U_n + C_n)}{D_n}$$

$$U_i = \frac{(U_i U_{i-1} + C_i)}{(U_i + U_{i-1})}, \quad i = 3, 4, \dots, n-1 \quad (9)$$

Therefore the solution starts from the free stream to the point near the wall and then marching by a step of δx and repeating the above procedure until completing the domain of solution.

3) TURBULENCE MODEL AND WALL PARAMETERS

The effective viscosity of a turbulent flow is assumed equal to the sum of the molecular viscosity and the eddy viscosity

$$\mu_{eff} = \mu + \mu_t$$

In the inner region of the turbulent boundary layer, the eddy viscosity is evaluated by mixing length model as :-

$$\mu_t = \rho L^2 \left| \frac{du}{dy} \right| \quad (10)$$

where L is the mixing length which is evaluated by a formula suggested by Cebeci [3] as follows:-

$$L = K (y + \Delta y) \left\{ 1 - \exp [-(y + \Delta y)/\Lambda] \right\} \quad (11)$$

where

$$\Lambda = \frac{26 \nu}{\left[\frac{\tau_w}{\rho} (1 + 11.8 p^+) \right]^{1/2}}$$

and Δy is the displacement in the y -coordinate due to surface roughness given by:

$$\Delta y = 0.9 \left(\frac{\nu}{U_r} \right) \left[(K_s^+)^{1/2} - K_s^+ \exp (K_s^+/6) \right] \quad (12)$$

where K_s is the equivalent sandgrain roughness height and

It is noticed that, Δy calculated by equation (12) is valid only for sandgrain roughness. Schlichting [1] deduced some correlations for relating any roughness K^* to sandgrain roughness K_s as :

$$K_s^+ = K^* \left(\frac{\lambda}{3.17} \right)^{0.08}; \quad 1 \leq \lambda \leq 4.68 \quad (13)$$

$$K_s^+ = E^+ \left(\frac{25}{\lambda} \right)^{4.72} ; \lambda > 4.60 \quad (14)$$

where λ is the roughness density parameter which is defined as the total surface area to the roughness area

In the outer region, the eddy viscosity is evaluated by

$$\mu_t = \gamma \rho \alpha U \delta^* \quad (15)$$

where

$$\alpha = \alpha_0 \left[\frac{(1 + 0.55)}{(1 + \pi)} \right]$$

α_0 is the value of α at $Re \geq 6000$, and

$$\pi = 0.55 \left[1 - \exp \left\{ -0.243 \pi^{1/2} - 0.298 \pi \right\} \right] \quad \pi = \frac{10}{425} - 1$$

and γ is the factor due to the intermittency of turbulence

in the outer region given by Cebeci [3] formula:-

$$\gamma = \left[1 + 5.5 \left(\frac{y}{\delta^*} \right)^2 \right]^{-1} \quad (16)$$

To calculate the wall shear stress, it is assumed that Couette flow near the wall is verified, for large values of y the viscous effect diminishes and the exponential term of the mixing length equation tends to zero. Thus the following equation can be deduced as:

$$U^+ = \frac{1}{K} \left[2 \left\{ (1 + P^+ Y^+)^{1/2} - 1 \right\} + \ln \left\{ \frac{4EY^+}{2 + P^+ Y^+ + 2(1 + P^+ Y^+)^{1/2}} \right\} \right] \quad (17)$$

where E is the wall parameter evaluated by

$$E = (0.577 + 81.677 P^+ - 965.91 P^{+2}) e^{-k \Delta u^+} \quad (18)$$

Δu is the downward shift of the velocity profile due to surface roughness and evaluated as:

$$\Delta U^+ = (2.44 \ln K_s^+ - 3.3) \sin[0.4258 (\ln K_s^+ - 0.811)]; K_s^+ \leq 90 \quad (19)$$

and

$$\Delta U^+ = 2.44 \ln K_s^+ - 3.3 ; 90 < K_s^+ \leq 2000 \quad (20)$$

Equation (17) is solved by iteration in the fully turbulent part where $y \geq 70$ or local $Re \geq 1100$.

By the same way Ilegbusi [10] integrated the energy equation and deduced an equation to calculate Stanton number

as follows:-

$$St = S / [Pr_t (1 + S^{1/2} P)] \quad (21)$$

where s is the shear stress coefficient and P is the laminar sub-layer resistance to heat transfer which was evaluated by Sapatelleke [11] as follows:-

$$P = 3.15 Pr_t^{0.005} \left(\frac{1}{E} - 0.116 \right)^{0.005} + 0.274 P_M E^{0.0} \quad (22)$$

$$\text{and } \frac{P}{M} = 9 \left(\frac{Pr_t}{Pr_t} - 1 \right) \left(\frac{Pr_t}{Pr_t} \right)^{1/4} \quad (23)$$

According to the experimental data that was carried out by Pimenta [12], the value of turbulent Prandtl number is taken equal to unity as shown in fig. (4).

The values of ω is used to calculate the values of normal distance y as follows:-

$$y_{i+1} - y_i = \frac{-1}{2} (\psi_{\kappa} - \psi_t) (\omega_{i+1} - \omega_i) \left[\frac{1}{(\rho u)_i} + \frac{1}{(\rho u)_{i+1}} \right] \quad (24)$$

The normal distance y_2 is calculated from a power velocity profile $(u/u_2) = (y/y_2)^b$

$$\text{where } b = \frac{\frac{u_z^*}{y_z^*} + \left[\left(\frac{Uz^*}{Yz^*} \right)^2 + 4K^2 U_z^{*2} (1 + Y_z^* P^*) \right]^{1/2}}{2K^2 U_z^{*2}} \quad (25)$$

$$\Psi_I = 1/(1+b) = \frac{\omega_z (\psi_{\kappa} - \psi_t)}{(\rho u)_z (y_2 - y_1)} \quad (26)$$

4 RESULTS AND DISCUSSIONS

In this section, the present prediction results are compared with the previously published data and simple Reynolds analogy factor correlations are predicted for turbulent flows over both smooth and rough surfaces subjected to zero and non-zero pressure gradients. The first station velocity and temperature profiles are used as the initial conditions to start the solution. The discrepancy between the experimental data and the present prediction results is expected. This is due to arise from the experimental errors, possible effect of three dimensionality of the actual flow, errors due to fitting the measured values of the free stream velocity distribution and the error due to reading the data.

from very small published papers.

4.1 Smooth Wall Computations:

The experimental data of Bell [13] are used to test the flow over smooth wall with zero pressure gradient. The solution starts at the leading edge at which the velocity and temperature profiles are uniform. Since the boundary layer thickness is equal to zero at the leading edge, thus this value is taken as 2mm to initiate the program. Figure (5) shows a comparison between the present prediction and the experimental data of both skin friction coefficient (C_f) and Stanton number (St). Also the present prediction of the momentum thickness (θ) and the displacement thickness (δ^*) are shown in the figure. It is noticed that the rates of increase for both (θ) and (δ^*) are linearly with streamwise direction (x). Maximum deviation for skin friction coefficient (C_f) is about 7 % and 3 % for Stanton number (St). This indicate excellent agreement between present and previously published results.

Another experimental data of Bell [13] are used to test the flow over smooth wall with negative pressure gradient. The free stream velocity distribution along the test surface is obtained by the least square curve fit of the measured values. Figure (6) shows a comparison between the present prediction and the experimental data of both skin friction coefficient (C_f) and Stanton number (St). Also the present prediction of the momentum thickness (θ) and the displacement thickness (δ^*) are shown in the figure. It is noticed that the rate of increase for both (θ) and (δ^*) is rapidly due to the rapid increase of Reynolds number and consequently the increase of turbulence level. The results of both (C_f) and (St) indicate good agreement between the present prediction and the measurements. The maximum discrepancy observed in (C_f) is about 12 % and in (St) is about 10 %.

Also the experimental data of Bell [13] are used to test

the flow over smooth wall with positive pressure gradient. The free stream velocity distribution along the test surface is obtained by the least square curve fit of the measured values. Figure (7) shows the measured values of both skin friction coefficient (Cf) and Stanton number (St) together with the present prediction results and the free stream velocity distribution. From the comparison between the present prediction and the measured values, it is shown that very good agreement of the present prediction is obtained. The maximum discrepancy in (Cf) is about 10 % and in (St) is about 8 % between the present prediction and measurements.

From the present computations, the following Reynolds analogy factor correlation is predicted as:

$$RAF = \frac{1}{1 - 2.952 \sqrt{Cf/2}} \quad (27)$$

4.2 Rough Wall Computations

The experimental data of Heazler [14] are used to test the flow of zero pressure gradient. The actual rough surface is composed of density packed spheres of uniform size with an equivalent roughness height. The temperature difference between the wall and the free stream is given in the range (10-15) C°. Figure (8) shows the measured and predicted values of (Cf) and (St) with the present prediction of (θ) and (δ^+) . The results indicate very good agreement. The slight deviation observed in both (Cf) and (St) is not greater than 5 %. The slope of (θ) and (δ^+) remain linear with streamwise direction x.

The experimental data of Coleman [15] are used to test the negative pressure gradient flow over rough surface. The free stream velocity distribution along the test surface is obtained by the least square curve fit of the measured values. Figure (9) shows a comparison between the present prediction and the measured values for both (Cf) and (St). Also the present prediction of (θ) and (δ^+) are presented in the figure. It is noticed that the rate of increasing (θ) and (δ^+) with the streamwise distance (x) is rapidly and

non-linear due to rapid increasing of turbulence degree. The comparison indicate good agreement in both (Cf) and (St) with the maximum discrepancy observed in (Cf) is about 5 % while in (St) is about 4 % . The discrepancy in (St) because of assuming that turbulent Prandtl number equal to unity, while its value is near to unity only close to the wall and it decreases to (.7 - .8) at the outer region but there is no mathematical model for this problem.

The experimental data of Parry and Joubert [16] serve as a test for flow over rough wall with positive pressure gradient. The heat transfer is not considered. The free stream velocity distribution along the test surface is obtained by the least square curve fit of the measured values. The initial velocity profile are generated from the given values of the data at the first station with Coles' wake parameter. Figure (10) shows the present prediction of (θ) and (Cf) with the measured values of (Cf) . The free stream velocity distribution is shown in the same figure. It is noticed that the rate of increase of (θ) and (δ^*) is less than that for zero pressure gradient flow due to decreasing of turbulence level for positive pressure gradient flow. The agreement in general, can be said to be good. The slight deviation observed are partly due to the uncertainty of the initial velocity profile and the inaccuracy of the data since they have been read from small plots.

Figure (11) shows the effect of surface roughness on Stanton number (St) for zero pressure gradient flow as $U=18.9$ m/s. From this figure it is noticed that for the same free stream velocity the increasing of roughness height will increase Stanton number and consequently the heat transfer rate. The curves of figure (11) are collapsed into a single curve as shown in figure (12) when they plotted against $(X-X_r)/K_s$. This mean that the heat transfer coefficient is inversly proportional to $(X-X_r)/K_s$. The same results are obtained for positive and negative pressure gradient flows as shown in figures (13), (14), (15) and (16). It is noticed that

for the same roughness effect, the heat transfer coefficient of accelerated flow is greater than that of zero pressure gradient flow and the heat transfer coefficient of zero pressure gradient flow is greater than that of decelerated flow.

Figure (17) and (18) shows the effect of surface roughness on the skin friction coefficient (C_f) for positive pressure gradient flows. Increasing the roughness height causes to increase the skin friction coefficient (C_f) as expected before.

From the present computations, the following Reynolds analogy factor is predicted

$$RAF = 2.5969652 - 535.95436 Cr + 37928.262 Cr^2 \quad (28)$$

where (C_f) for rough surface subjected to pressure gradient is given by

$$C_f = \left[L + M \text{Log} \left[\frac{X - X_r}{K} \right] \right]^{-2} ; \frac{X - X_r}{K} \geq 50$$

Where L and M are given by

$$L = 7.5 - 3a \quad , \quad M = 2.123 - 0.42 a + 54 a^2$$

where a is constant smaller than (-0.333)

5 CONCLUSIONS

The two dimensional hydrodynamic and thermal turbulent boundary layer equations are solved numerically by using Spalding - Patanker ($x-\omega$) coordinate system and a finite difference method with 4-node implicate formula. The modified turbulence model is used with a modified wall function to including the effect of pressure gradient and surface roughness. A special calculation of the normal distance near the wall is also used in the present method. Several flows over smooth and rough surfaces with and without pressure gradients are computed by the present prediction method. Results obtained have shown very good agreement with experimental data. Both skin friction coefficient C_f and Stanton number St are increases with surface roughness as

expected from the previous published works. An increase also is obtained with accelerated flow as compared with constant free stream velocity and decelerated flows.

NOMENCLATURE

- A Van Driest damping factor
 A^* Normalized damping factor = $A \text{ ur} / \mu$
 A_i Coefficient in the finite difference equations
 a Term expressing mass transfer through I - boundary
 B_i Coefficient in the finite difference equations
 b Term expressing rate of increase of fluid in boundary layer
 b Constant
 C_i Coefficient in the finite difference equations
 C_f Skin friction coefficient = τ_w (shear stress at wall) / $\frac{1}{2} \rho U_\infty^2$
 c Transport property
 c_p Specific heat at constant pressure
 D_i Coefficient in the finite difference equations
 d Source term
 E Wall parameter
 k Normal height of roughness element
 k^+ Roughness Reynolds number = $k U_\tau / \nu$
 K_s Sandgrain roughness height
 K_s^+ Sandgrain roughness Reynolds number
 L Mixing length
 \dot{m} Rate of mass flow across grid lines per unit area
 N Total number of cross - stream node points
 P Pressure
 P Laminar sub-layer resistance to heat transfer
 Pr Prandtl number
 Pr_t Turbulent Prandtl number
 p^* Normalized pressure gradient term = $\frac{\nu}{\rho U_\tau} \frac{dP}{dx}$
 P_i Coefficient in the modified form of the finite difference equation
 Q_i Coefficient in the modified form of the finite difference equation

120
int

Re Reynolds number
Re_l Local Reynolds number = yu/ν

Si Source term

St Stanton number

Ti Term representing diffusive effects in the finite difference equations

U Free stream velocity

u Local velocity through the boundary layer

u* Shear velocity = $\sqrt{\tau_w / \rho}$

u* Normalized local mean velocity = u/u^*

z Downward shift of velocity profile due to roughness

x Streamwise distance from the leading edge

xr Streamwise distance measured from roughned part

y Normal distance to the wall

zy Displacement in y - coordinate due to roughness

y* Normalized distance = yur / ν

δ Boundary layer displacement thickness

δ Boundary layer momentum thickness

λ Roughness density parameter

μ Fluid viscosity

μ_t Turbulent (eddy) viscosity

μ_{eff} Effective viscosity

k_{eff} Effective thermal conductivity

c_{eff} Effective exchange coefficient

α Eddy viscosity parameter

ν Kinematic viscosity

ρ Fluid density

θ Typical dependent variable

ψ Stream function

ψ₀ Special stream function parameter

ω Dimensionless stream function parameter

γ Intermittency factor

Subscripts

I Inlet

E Exit

REFERENCES

- [1]- Schlichting, H., "Boundary layer theory", Mc-Graw-Hill, New-York, 1968.
- [2]- Hinze, J.O. "Turbulence". Mc Graw-Hill. New York, 1975.
- [3]- Cebeci, T.; and Chang, K.C., "Calculation of incompressible rough wall boundary layer flows" AIAA J. Vol 10, pp. 730-735, 1978.
- [4]- Dvorak, f.a., "Calculation of compressible turbulent boundary layer with roughness and heat transfer". AIAA J. Vol 10, pp. 1447-1451, 1972.
- [5]- Dvorak, f.a., "Calculation of turbulent boundary layers on rough surfaces in pressure gradient". AIAAJ. Vol 7, pp. 1752-1759, 1969.
- [6]- Cebeci, T., "Behaviour of turbulent flow near a porous wall with pressure gradient". AIAAJ. Vol 8, pp. 2152-2156, 1970.
- [7]- Spalding, D. B., "GENMIX-A general computer program for two dimensional parabolic phenomena". Program press, 1977.
- [8]- Mahmood, K.M., "The prediction of smooth and rough wall turbulent boundary layers in pressure gradient". M Sc, Thesis, University of Mosul, 1978.
- [9]- Abd-Rabbo, M. F., "Aerodynamics drag of ridges arrays in adverse pressure gradient", Ph. D. Thesis, Leicester University, 1977.
- [10]- Ilegbusi, J.O., "Proposal for wall function for friction and heat transfer in the presence of roughness and mass transfer", Int, Comm, Heat Mass Transfer, Vol. 11, pp. 569-581, 1984.
- [11]- Jayatilaka, C.V. L., "The influence of Prandtl number and surface roughness on the resistance of the laminar sublayer to momentum and heat transfer", program press, Vol 1, pp 193-330, 1969.
- [12]- Pimenta, M.H., "The turbulent boundary layer : An experimental study of the transport of momentum and heat with the effect of roughness". Ph.D. Thesis. Stanford University, 1975.

- [13]-Coles, D.E.; and Hirst, E.A. (Editor), "Proceeding computations of turbulent boundary layers", Vol 11. Stanford University, 1968.
- [14]-Christoph, G.H., "Skin friction and heat transfer for combined roughness and mass addition", ASME Publication FED. Vol 11, 1984
- [15]-Coleman, R.J., "Characteristics of turbulent boundary at low Reynolds numbers with and without transpiration" J. Fluid Mech. Vol 42, pp. 769-802, 1970.
- [16]-Perry, A.E.; and Joubert, P.N., "Rough wall boundary layers in adverse pressure gradient", J. Fluid Mech. Vol 17, pp. 193-211. Oct. 1963.

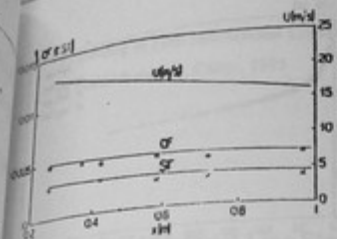


Figure 10) Comparison between present prediction and Bell's data.

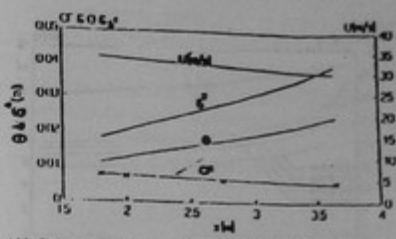


Figure 10) Comparison between present prediction and results Perry and Joubert's data, Ref. [16]

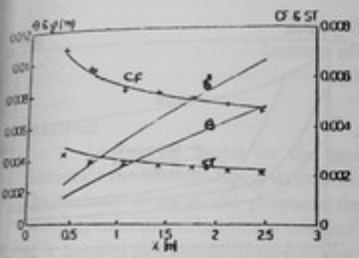


Figure 11) Comparison between present prediction and results for Reize's data, Ref. [14]

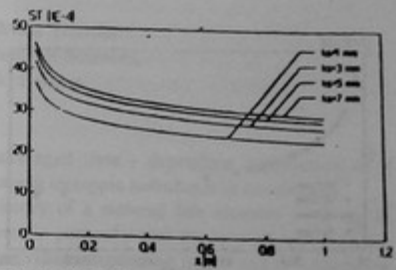


Figure 11) The effect of roughness height on Stanton number for zero pressure gradient flow

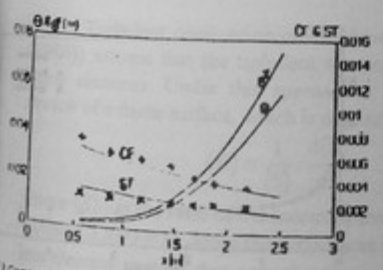


Figure 12) Comparison between present prediction and Coleman's data, Ref. [15]

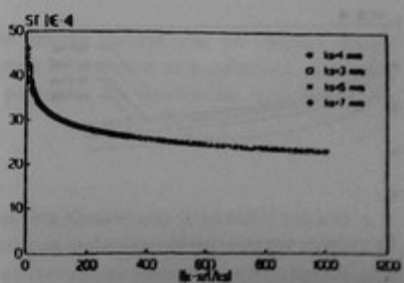


Figure 12) The Collapse curve of [ST] for zero pressure gradient flow on rough surface

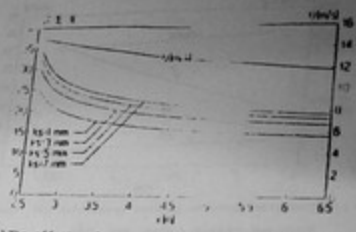


Figure (15) The effect of positive pressure gradient flow and UFF gradient flow on rough surface roughness height on Stanton number [ST]

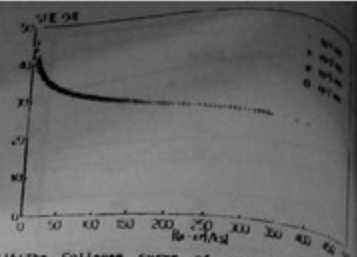


Figure (16) The Collapse curve of [ST] for negative pressure gradient flow

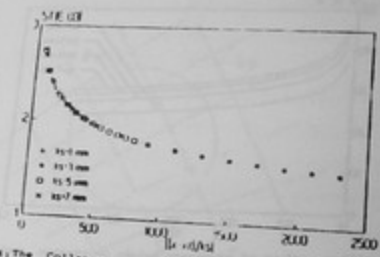


Figure (17) The Collapse curve of [ST] for positive pressure gradient flow on rough surface

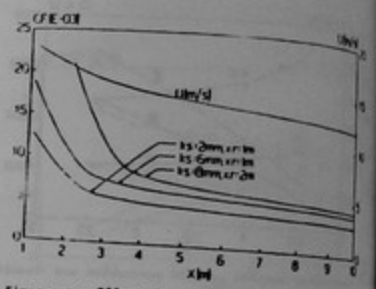


Figure (18) Effect of roughness height $[k_s]$ on [ST]

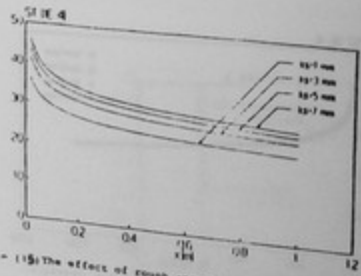


Figure (19) The effect of rough negative pressure gradient flow on Stanton number [ST]

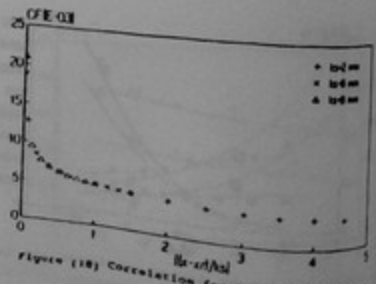


Figure (20) Correlation for friction coefficient